Preprint
UCRL-JC-141084

3D HYDRA Simulations of NIF Targets

M. M. Marinak, G. D. Kerbel, N. A. Gentile, O. Jones, S. Pollaine, T. R. Dittrich, S. W. Haan

This article was submitted to the 42nd Annual Meeting of the APS Division of Plasma Physics, Quebec City, Canada, October 23-27, 2000

U.S. Department of Energy
Lawrence Livermore National Laboratory

October 20, 2000

DISCLAIMER

This work was performed under the auspices of the United States Department of Energy by the University of California, Lawrence Livermore National Laboratory under contract No. W-7405-Eng-48.

3D HYDRA simulations of NIF targets

M. M. Marinak, G. D. Kerbel, N. A. Gentile, O. Jones,
S. Pollaine, T. R. Dittrich, S. W. Haan
Lawrence Livermore National Laboratory
(October 20, 2000)

Abstract

The performance of NIF target designs is simulated in three dimensions using the HYDRA multiphysics radiation hydrodynamics code. In simulations of a cylindrical NIF hohlraum that include an imploding capsule, the motion of the wall material inside the hohlraum shows a high degree of axisymmetry. Laser radiation is able to propagate through the entrance hole for the required duration of the pulse. Gross hohlraum energetics in the simulation mirror the results from an axisymmetric simulation. A simulation of a copper-doped beryllium ablator NIF capsule carried out over large solid angle resolved the full spectrum of the most dangerous modes that grow from surface roughness. Hydrodynamic instabilities evolve into the weakly nonlinear regime. There is no evidence of low mode jetting driven by nonlinear mode coupling.

I. INTRODUCTION

The National Ignition Facility, under construction, is a 192 beam frequency tripled ($\lambda = 0.35\mu m$) Nd:glass laser system designed to generate shaped pulses delivering 1.8 MJ at a peak power of 500 TW. Assuming the NIF laser performs according to specifications, detailed computer simulations [1–8] have identified a variety of indirectly-driven target designs which can achieve ignition. These achieve ignition over energies ranging from 0.9 to 1.8 MJ with the range of peak drive temperatures varying from 250 to 400 ev. These designs employ a cylindrical hohlraum which converts laser light to x-rays, resulting in a more symmetric radiation flux onto the capsule. The hohlraum gas-filled in order to limit the motion of the high atomic number wall material. The large number of beams on NIF are intended to produce a nearly axisymmetric radiation flux onto the capsule. A great deal of hohlraum design work has been done using the axisymmetric 2-D multiphysics radiation hydrodynamics code LASNEX. [9] However there are a number of issues we would like to examine with direct 3-D simulations. The possibility that the discrete nature of the laser spots results in a 3-D wall motion that affects the symmetry of the capsule implosion, either by affecting the radiation flux or by hydrodynamic jetting. If jetting in 3-D was large enough thermal conduction could communicate temperature asymmetries in the channel to the capsule, adversely affecting implosion symmetry. We would also like to verify the ability to keep the laser entrance hole open in the absence of an axisymmetric illumination pattern. A direct 3-D simulation allows us to calculate the radiation flux on the capsule taking into full account such effects as wall motion, laser spot broadening. albedo variations and volumetric emission from the hohlraum channel.

In addition to the asymmetry caused by the radiation drive, perturbations on the capsule surfaces seed hydrodynamic instabilities, which can cause shell breakup and quench capsule ignition. For a broad range of modes the growth factors due to hydrodynamic instabilities are sufficiently large that perturbations progress into the nonlinear regime, where saturation effects and mode coupling are important. The higher nonlinear saturation amplitudes obtained in three dimensions are well established. cite[Trygvasson, ...,Dahlburg, Shvarts, Marinak] In addition to assessing the capsule's ability to withstand the larger amplitudes we wish to examine the effects of nonlinear mode coupling in the presence of the full spectrum of modes. Is nonlinear mode coupling between high order modes able to generate low mode asymmetries which could threaten ignition.

This article gives examples of how we are using HYDRA to simulate in three dimensions many of these aspects of NIF target performance. The remainder of this article is organized as follows. In Section II we describe HYDRA. A description of the hohlraum simulation results is presented in Section III. We discuss in Section IV results from a highly resolve, large solid angle simulation of hydrodynamic instabilities on a NIF ignition capsule.

II. HYDRA

HYDRA is a 2D and 3D multiphysics radiation hydrodynamics code. It now has the physics required for simulations of NIF targets. HYDRA is based upon ALE hydrodynamics. A variety of grid motion algorithms are available, including weighted equipotential relaxation. The code makes use of modern monotonic artificial viscosities. Second order monotonic advection are performed on scalar fields and momentum. Material interfaces are resolved using interface reconstruc-

tion. cite[youngs] HYDRA includes a laser raytrace and deposition package. Several deposition models are available, including the default inverse Brehmstrahlung. Ray orbits are calculated with second order accuracy. A new heavy ion deposition package is operational. Radiation transport is handled either with Monte Carlo photonics or with flux limited multigroup diffusion. As of this writing the Monte Carlo photonics package does not yet function in problems with material interfaces. This is expected to be handled soon. A variety of LTE and NLTE opacity models are available, including inline XSN cite[xsn], and the newly developed Linear Response Matrix Opacity method for NLTE opacities cite[lrm]. An online server allows LTE opacity tables to be generated for arbitrary mixtures. Thermonuclear burn is treated, included multigroup charged particle transport and isotope production and depletion. Neutron energy deposition can be treated adequately in the free streaming limit for ICF capsules, which are thin to neutrons. Electron and ion conduction are treated using flux-limited finite element operators. Conductivities and electron-ion coupling coefficients are obtained from the model of Lee and More cite[more]. A variety of methods are available for solving matrices which arise from the operator splitting employed. For large matrices two multigrid methods are available from the HYPRE cite[falgout] solver library. This method is fully scaleable for large problems as the iteration count for the multigrid method is insensitive to the problem size. The multigrid methods can be used directly or as a preconditioner to the conjugate gradient solver. Many equations of state are available, including the inline Quotidian equation of state (QEOS), the EOS IV tabular data base, Sesame tables and the LEOS library.

HYDRA has been modified to run on distributed clustered (shared memory parallel) SMP architectures. It makes use of a strategy based upon POSIX threads, OpenMP and the MPI message passing library. All of the physics packages now run in a distributed parallel mode where domains are handle by individual nodes of the platform. HYDRA has demonstrated high parallel performance on problems using up to 1680 processors of the ASCI cite[asci] machine at Lawrence Livermore National Laboratory.

The hydrodynamics and physics packages in HYDRA have been tested extensively. HYDRA has also been tested against many types of laser-driven experiments cite[marinakprl95,marinak97,marinakprl98,...].

III. HOHLRAUM SIMULATIONS

We first consider a scale 0.6 hohlraum which was designed for the 96 beam configuration initially planned for NIF. A schematic of the target is shown in figure ref[hohlfig]. The hohlraum measures 6.0 mm long by 3.3 mm in diameter. A gas fill mixture of equal amount of He-H at 6.e-4 g/cm3 is intended to tamp the motion of the hohlraum wall material. This is intended to prevent jetting to the center of the hohlraum, and resulting asymmetries in the capsule implosion. A 0.8 mm thick polyimid window on each laser entrance hole maintains the gas fill. The hohlraum wall is fabricated from a mixture of equal amounts of U-Pb-Ta-Dy-Nb. This "cocktail" mixture has lines overlapping, producing a higher average opacity. These mixtures result in higher energy conversion efficiency than pure gold hohlraums. cite[orzechow] A plastic liner 0.8 μm thick covers the wall material at the laser entrance hole. The capsule employs a polyimid ablator (CHNO) 95 mm thick enclosing a cryogenic layer of DT 48 μm thick. The central region contains DT gas at a density of 0.3 mg/cm3.

We simulated 1/4 of the hohlraum, enforcing symmetry at the boundaries. The vol-

ume simulated extends 180 in azimuth and to the symmetry plane at the equator. The simulation includes all of the features of the hohlraum described above. For the purposes of this simulation the hohlraum was illuminated using the 192 beam pattern of full NIF. Light comes into the laser entrance hole in two cones. The quarter hohlraum is itself illuminated by 12 beam groups, each representing 4 beams. Eight of these groups are associated with the outer cone. Each beam is represented in the laser package as a Gaussian ellipse, with 300 rays per beam. The relative power in these cones is dynamically varies to minimize the time-varying pole-to-waist asymmetry, which is described as a P2 Legendre polynomial. The simulation employed inline XSN LTE opacities ref[xsn], the quotidian equation of state /ref[qeos]. At the time of this writing the Monte Carlo photonics package did not yet function with the material interface tracker. This simulation was performed using multigroup radiation diffusion. In the cylindrical hohlraum the 3-D components of asymmetry arise entirely from the laser spots. The gross energy losses from the hot spots, due to electron conduction and radiation emission, are expected to be calculated reasonably accurately with this model.

The laser pulse has a length of 10.0 ns. The beams deposit energy in two pairs of rings. The inner pair of these rings is composed of beams aimed at 23.5 and 30 degrees to the hohlraum axis, and the other has beams at 44.5 and 50 degrees. The inner cone beams in this simulation have elliptical focal spot widths of 189 by 356 μm, while the outer cone beams have a focal spot measuring 347 by 388 μm.

This particular design is not intended to ignite the capsule, which produces a yield of 4 kJ.

Fig. 2a-c shows the electron temperature contours on a cut-away view showing a mesh surface on the hohlraum at three times. The laser beams burn through the polyimid window and then into the gas for 900 ps before the outer ring begins heating the wall appreciably. Initially individual laser spots are visible, but laser spot broadening quickly converts the contours at the outer rings into a true ring pattern. The beams forming the inner ring reach the wall at 2.2 ns. The inner ring has half the number of beams around its circumference as the outer spots. The laser hot spots in the inner ring remain more distinct than for the outer ring.

Fig. 3a-c plots the motion of the different material regions on the boundaries of the simulated volume for three times. The plastic liner in the around the laser entrance hole is intended to prevent the hohlraum wall material from filling the hole, so that the laser energy is delivered into the hohlraum interior. The plots show the plastic liner filling the hole. It succeeds in keeping the hole open for the required duration of the laser pulse. The hole closes by the last time shown, after the required energy has been delivered and the capsule has fully converged.

An examination of the density profile in the interior of the hohlraum shows that the gas is effectively tamping the wall motion. The density profile shows only slight deviations from axisymmetry. These variations are largest in the vicinity of the laser entrance hole. The energetics from this hohlraum have been compared with a 2-D axisymmetric simulation. The radiation temperature within the hohlraum is nearly identical between the two, indicating that the laser energy is coupling was not degraded in 3D.

The use of radiation diffusion results in a radiation flux onto the capsule that is artificially symmetric. This calculation effectively tests the ability of the code to maintain the symmetry of the capsule. Fig. 4 shows the spherical density contours of the capsule at 10.25 ns, after it has converged by a factor of 30 xxx. Asymmetries caused

by the hohlraum can also be communicated to the capsule hydrodynamically or through thermal conduction. The high degree of capsule symmetry shows that these mechanisms are not playing any important role in the simulation.

The Radiation the flux onto the capsule can be calculated by postprocessing the 3D hohlraum simulations. The flux on the capsule is obtained by solving the transport equations directly on rays which foliate 2pi solid angle at locations on the capsule surface. This method takes into account the effect of capsule convergence.

Three-dimensional components of asymmetry can also be calculated using a viewfactor code. Calculations done with the viewfactor code allow for the time variation in the wall albedo and also take into account the capsule convergence. But the viewfactor analysis lacks potentially important effects such as volumetric emission and laser spot broadening due to thermal conduction.

We have calculated the intrinsic radiation flux from the quarter hohlraum simulation. This simulation geometry introduces two approximations into the illumination pattern due to the symmetry planes at the equator and at the azimuthal extents of the mesh. The former is equivalent to rotating the beams opposite the equator to obtain symmetry. This changes the illumination pattern, reinforcing the laser spots in the inner ring compared with the actual NIF geometry. We have compared coefficients for the significant spherical harmonic modes obtained with the two approaches outlined. For the effective illumination geometry of this simulation these modes are Y44, Y64, Y84 and Y88. In spite of the effects missing from the viewfactor code results show 3-D asymmetry coefficients obtained from the hohlraum simulations are similar. The two methods produce a similar picture of the 3-D intrinsic radiation asymmetries in this problem. These techniques give us the capability to calculate radiation flux inside the hohlraum from a direct 3-D simulation. We can impose this radiation flux on the capsule and assess its effect on implosion symmetry. In the future we will employ these techniques in full hohlraum simulations using the exact NIF illumination geometry.

IV. HYDRODYNAMIC INSTABILITIES

One issue we wish to assess is the ability of the capsule to withstand the growth due to hydrodynamic instabilities of perturbations with realistic 3-D shapes. These saturate at larger amplitudes in three dimensions. cite[marinak,dahlburg,shvarts...] The higher nonlinear saturation amplitudes in 3-D could lead to mode coupling effects in 3-D which are more pronounced than in 2-D. We are interested in simulating the growth of the full spectrum of dangerous modes to assess whether any anomalous low mode jetting occurs due to an inverse cascade via mode coupling.

In addition to the asymmetry caused by the radiation drive, we perform highly resolved capsule only simulations of hydrodynamic instabilities.

We consider a capsule which employs a beryllium ablator doped with 0.9Its design parameters were specified by Dittrich. [4]. Earlier beryllium capsule designs were produced by Wilson [3] and Levedahl. [1] The ablator is 135 μm thick, extending to an outer capsule radius of 1085 μm. Dopants in the ablator shields the fuel from x-ray preheat and helps to control the reduce the Atwood number at the ablator-fuel interface. The latter effect helps to reduce small scale instability growth there. The cryogenic DT ice region extends inside of the ablator 80 μm, enclosing a region of DT gas in equilibrium with the ice. It is driven by a shaped pulse, with

a peak temperature of 300 ev produced by the full 192 beam configuration of NIF. The laser power history used to drive this capsule has four steps. Each of these steps launches a shock during the implosion of the capsule. In order to maintain the fuel on a low adiabat it is important that the shocks do not join until they have broken into the DT gas.

We study hydrodynamic instability growth by performing a highly resolved simulation of a subset of the capsule solid angle. Advances in the computer power available under the ASCI program cite[asci] have enabled us to model considerably larger solid angles then was practical before. cite[marinak98]. In the simulation we consider here the domain extends from -36 to +36 degrees in latitude and 72 degrees in longitude. Reflection boundary conditions are employed at the transverse boundaries. The mesh measured 360 x 360 x 171 zones in the two transverse directions and radial direction respectively. This gives 18 zones per transverse wavelength for mode l = 100.

For this ignition capsules the tolerances for surface roughness is most restrictive for the outer ablator and inner ice surfaces. cite[dittrich,marinak,wilson]. We initialized the perturbations on the gas-ice surface based upon laboratory measurements. [10] The surface perturbations can be were described with a functional form:

$$R_{lm}(cm) = \frac{1.e^{-4}}{3l^{0.6} + 2.2 \times 10^{-7} l^4}$$

where R_{lm} is the spherical harmonic perturbation amplitude in centimeters and l is the perturbation mode number. Recent work on this surface and its characterization shows smaller mode amplitudes than were used here.

A variety of methods for producing doped Be ablator capsules are being developed. In one approach the BeCu is sputter deposited onto a mandrel. [11] In another hollow BeCu hemispheres are brazed together and machined into a sphere. [12] Beryllium fabrication through a chemical vapor deposition process is also under research. [13] Since the fabrication techniques are presently under development the characteristics of surfaces achieved in fabricating Nova plastic were used to estimate the mode spectrum of the BeCu spheres. The mode spectrum can be described with the form:

$$R_{lm}(cm) = \frac{20}{l^{1.5}} + \frac{0.16}{(\frac{l}{60})^{0.7} + (\frac{l}{1200})^4},$$

where R_{lm} is the perturbation mode amplitude in nanometers and l is the perturbation mode number.

Modes with l=2-100 were initialized in the simulation. Above l=100 the product of amplitude with growth factor is small enough that they should make only a small contribution to the resulting ablation front rms. Previous 2-D multimode simulations which included modes up to l=160 supported this conclusion. Thus this simulation is able to resolve simultaneously the full spectrum of the most dangerous modes which arise from surface roughness. The imposed perturbations have the form

$$G(\theta, \phi) = \sum_m \sum n a_{mn} cos(\frac{m\pi\theta}{\Delta\theta}) cos(\frac{n\pi\phi}{\Delta\phi}),$$

where a_{mn} is the mode coefficient. The power in the 3D spectrum is summed into bins and distributed to the discreet modes supported which have the closest effective l values. Random phasse factors are assigned to a_{mn} so that the topology of the surface does not have uncharacteristically large peaks and valleys. Contour plots of the actual perturbations initilized on the surfaces are shown in Fig. 3a,b.

Fig. 4 shows two iso-density contour surfaces from the simulation at 15.55 ns. These surfaces are in the ablator and the boundary of the inner capsule wall. The prominent

bubbles and spike sheets growing in the ablation front have l=60-90. Fig. 5 shows similar surfaces at 15.65 ns, after the capsule has reached peak implosion velocity. The ratio of amplitude to wavelength in the ablator has increased largely due to the effect of convergence. The basic perturbation pattern persists through the implosion phase, indicating weakly nonlinear behavior. For implosions which successfully ignite, as does the present example, bubble merger [?] is not a prominent feature in ablation front evolution. These high modes growing in the ablator can threaten shell integrity during the implosion phase, when the shell is thinnest, if they breach the shell integrity before the capsule reaches peak implosion velocity. In spite of the apparently large amplitudes in the ablator these perturbations can no longer reach the inside of the capsule as it is rapidly thickening to convergence. Bubbles rising into the inner shell surface have a much lower typical mode number, falling in the range l = 10-20. The topology of the growing perturbations remains similar across the solid angle. There is no indication of significant low mode asymmetries driven by mode coupling. The amplitudes and mode numbers that describe the dominant features in the capsule shell resembled results from previous 3D simulations performed over a 12 degree wedge with similar amplitudes. cite[marinak98]. This result indicates the smaller simulations with a limited range of modes (l=15-120) was able to model the essential nonlinear dynamics of the instability growth.

As the capsule converges the fuel bubble grow in the presence of conductive stabilization from the hot spot. The average mode number of the bubble drops with time, approaching l=10. (Fig. 5?) This is not

Fig. 6 shows the capsule shell very late, after it/the high density fuel has begun burning vigorously. The capsule has produced a yield of 1 MJ at this time. By this time bubbles of fuel that have penetrated the shell are apparent. Although fuel is escaping through these bubble, the burn occurs so rapidly that they cannot have a significant effect on the yield. The total yield for this capsule is 15.4 MJ, compared with a 1-D clean yield of 17.0 MJ.

V. CONCLUSIONS

We are now able to simulate many aspects of NIF target performance in 3D using HYDRA. Initial simulations of gas filled cylindrical hohlraums, including the capsule implosion, showed gas fill effectively tamped the hohlraum wall motion. The wall motion inside the cylindrical hohlraum showed little deviation from axisymmetry. The largest deviations from axisymmetry in the density occurred in the plane of the laser entrance hole. For parameters used in these calculations the laser entrance hole did remain open for the required duration of the laser pulse. For the parameters of this simulation the radiation temperature in the hohlraum was essentially identical to the result for an equivalent 2D axisymmetric simulation performed with HYDRA. Using results from the hohlraum simulation simulation, we are now able to calculate the 3D radiation flux onto the capsule, by integrating the transport equations directly along rays from locations on the capsule.

Results for the approximation to the NIF illumination geometry made in this simulation produced a similar picture of the intrinsic 3D asymmetries in the hohlraum as obtained from our viewfactor code.

We presented results from a highly resolved, large solid angle simulation of a NIF capsule with a copper-doped beryllium ablator. The simulation resolved the growth of the full spectrum of the most dangerous modes caused by surface roughness. The amplitudes and mode numbers which describe the dominant features in the capsule shell re-

sembled results from previous 3D simulations performed over a much smaller solid angle. The simulation showed no evidence of significant low mode asymmetries driven by mode coupling. With rms roughnesses of 20 nm for ablator and 1.0 μm for the ice respectively the capsule gave a yield of 15.4 MJ compared with a clean 1-D yield of 17.0 MJ. The presence of bubbles of fuel penetrating through the capsule during the burn phase did not substantially reduce the yield.

ACKNOWLEDGEMENTS

This work was performed under the auspices of the U.S. Department of Energy by the University of California Lawrence Livermore National Laboratory under contract W-7405-Eng-48.

REFERENCES

[1] J. D. Lindl, Phys. Plasmas **2**, 3933 (1995)

[2] S. W. Haan, S. M. Pollaine, J. D. Lindl, L. J. Suter, R. L. Berger, L. V. Powers, W. E. Alley, P. A. Amendt, J. A. Futterman, W. K. Levedahl, M. D. Rosen, D. P. Rowley, R. A. Sacks, A. I. Shestakov, G. L. Strobel, M. Tabak, D. B. Harris, N. M. Hoffman, and B. H. Wilde, Phys. Plasmas **2**, 2480 (1995).

[3] W. J. Krauser, N. M. Hoffman, D. C. Wilson, B. H. Wilde, W. S. Varnum, D. B. Harris, F. J. Swenson, P. A. Bradley, S. W. Haan, S. M. Pollaine, A. S. Wan, J. C. Moreno, P. A. Amendt, Phys. Plasmas **3**, 2084 (1996).

[4] T. R. Dittrich, S. W. Haan, S. Pollaine, A. K. Burnham, G. L. Strobel, Fusion Tech. **31** (4) (1997).

[5] T. R. Dittrich, S. W. Haan, M. M. Marinak, S. M. Pollaine, and R. McEachern, Phys. Plasmas **5**, 3708 (1998).

[6] T. R. Dittrich, S. W. Haan, M. M. Marinak, S. M. Pollaine, D. E. Hinkel, D. H. Munro, C. P. Verdon, G. L. Strobel, R. McEachern, R. C. Cook, C. C. Roberts, D. C. Wilson, P. A. Bradley, L. R. Foreman, and W. S. Varnum, Phys. Plasmas **6**, 2164 (1999).

[7] D. C. Wilson, P. A. Bradley, N. M. Hoffman, F. J. Swenson, D. P. Smitherman, R. E. Chrien, R. W. Margevicius, D. J. Thoma, L. R. Foreman, J. K. Hoffer, S. R. Goldman, S. E. Caldwell, T. R. Dittrich, S. W. Haan, M. M. Marinak. S. M. Pollaine, J. J. Sanchez, Phys. Plasmas **5**, 1953 (1998).

[8] M. M. Marinak, S. W. Haan, T. R. Dittrich, R. E. Tipton, G. B. Zimmerman **5**, 1125 (1998).

[9] G. B. Zimmerman and W. L. Kruer, Comments Plasma Phys. Control. Fusion **2**, 51 (1975).

[10] J. K. Hoffer, L. R. foreman, J. J. Sanchez, E. R. Mapoles, and J. D. Sheliak, Fusion Technol, **30**, 529 (1996).

[11] R. McEachern, C. Alford, R. Cook, D.

Makowiecki, R. Wallace, Fusion Technology, **31** 435 (1997).

[12] Margevicius, R.W.; Salzer, L.J.; Salazar, M.A.; Foreman, L.R., *Twelfth Target Fabrication Specialist' Meeting (TFM'98)*, Jackson Hole, WY, 19-23 April 1998; Fusion Technology, **35** 2:106-14 (1999).

[13] K. V. Salazar, S. G. Patillo, M. Trkula, *Proceedings of the Thirteenth Target Fabrication Meeting*, Catalina Island, CA 8-11 November 1999, in press.

[14] U. Alon, D. Shvarts, and D. Mukamel, Phys. Rev. E **48, 1008 (1993); Phys. Rev. Lett. 72, 2867 (1994).**

U-Pb-Ta-Dy-Nb cocktail hohlraum

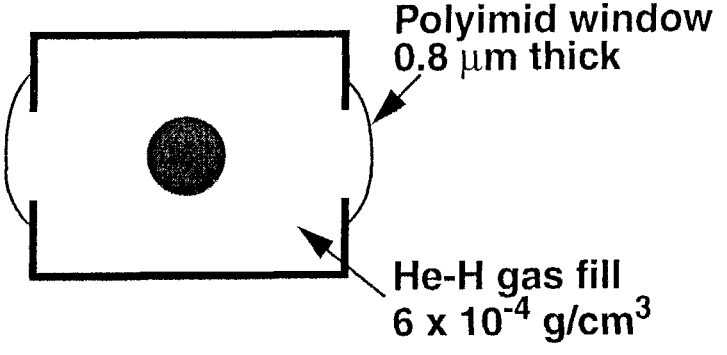

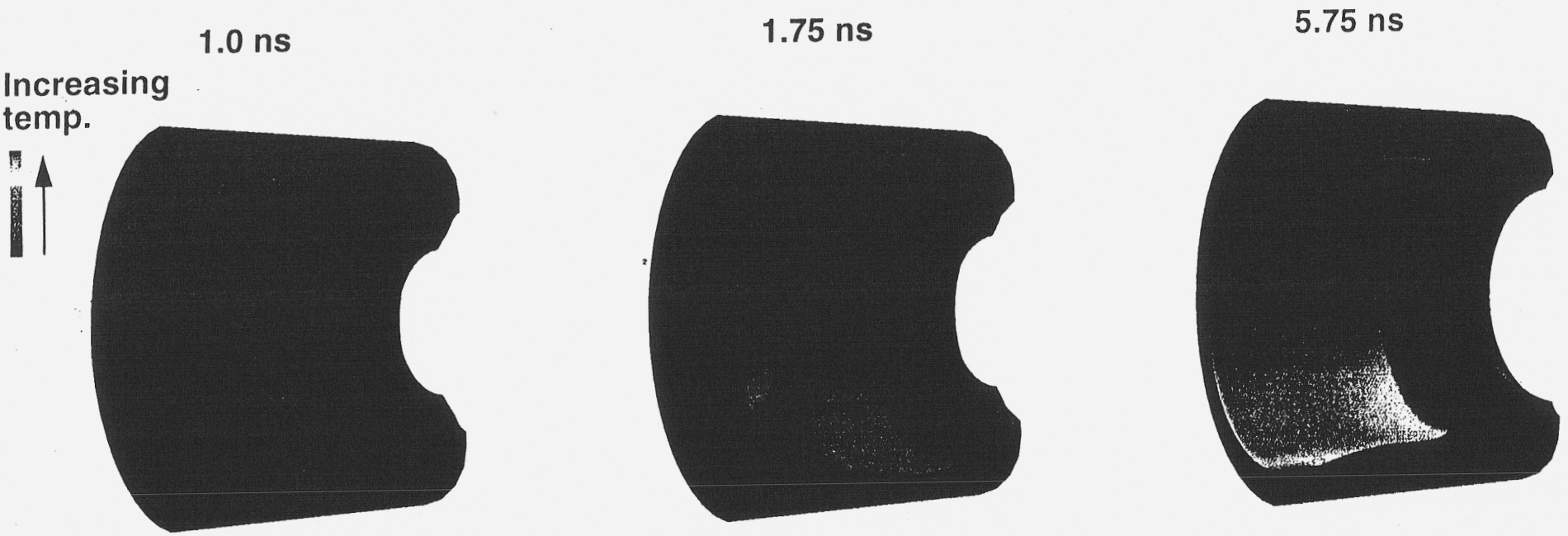
1.0 ns
1.75 ns
5.75 ns
Increasing
temp.

1.0 ns

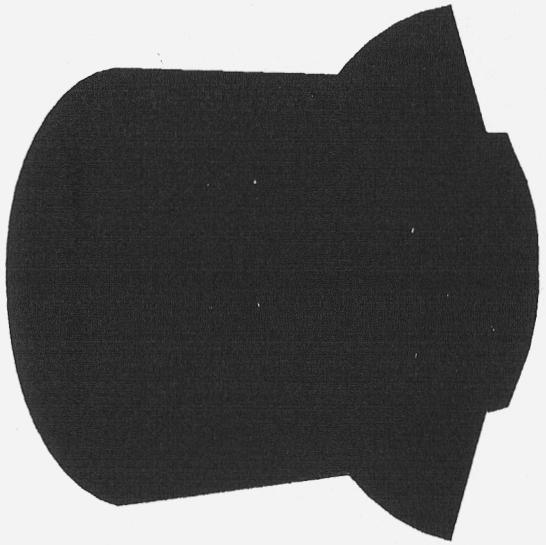

7.0 ns

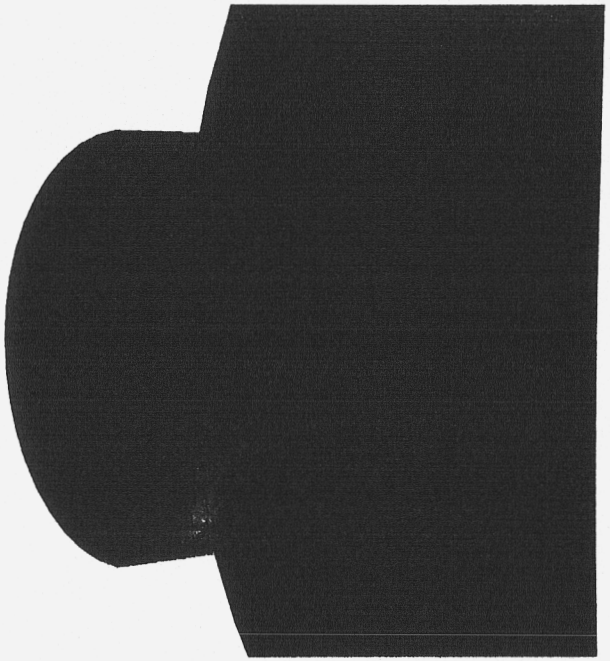

10.25 ns

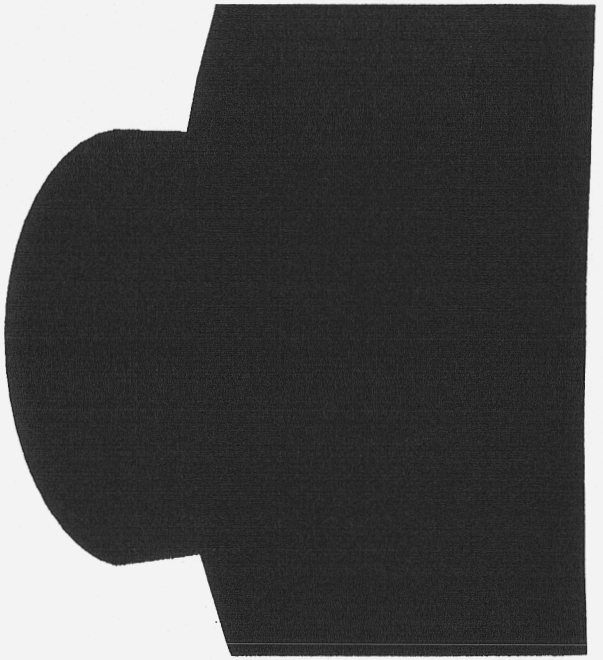

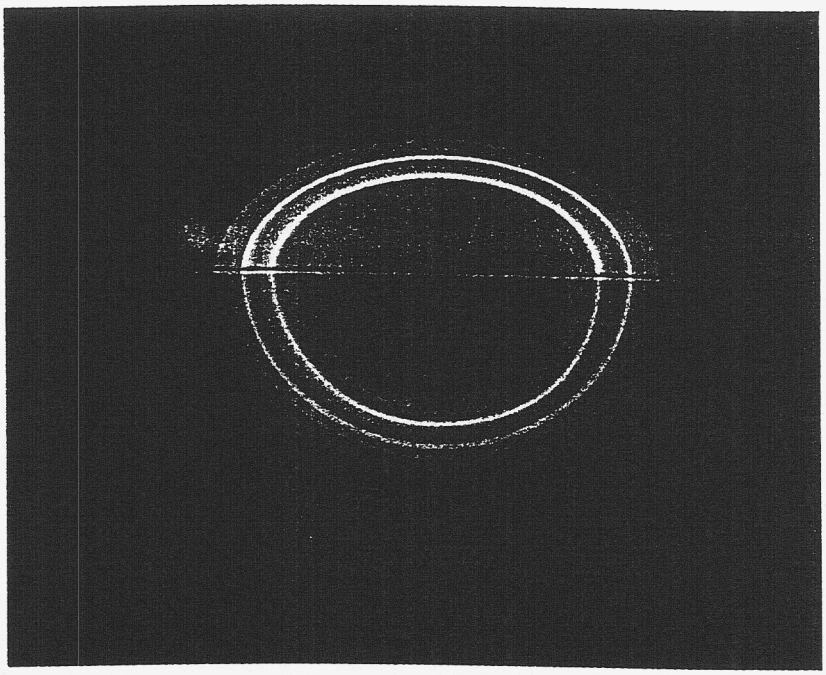

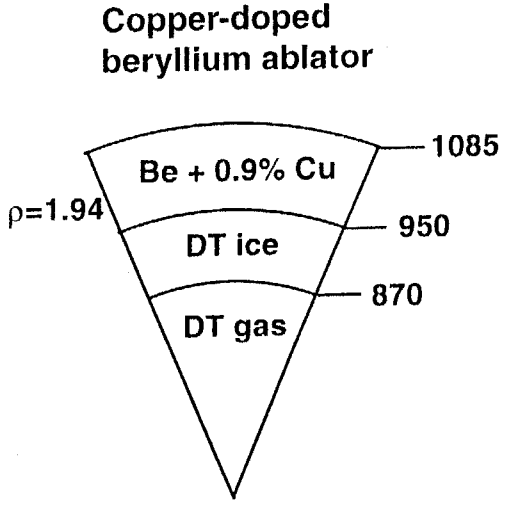
Copper-doped
beryllium ablator
Be + 0.9% Cu
ρ=1.94
DT ice
DT gas
1085
950
870

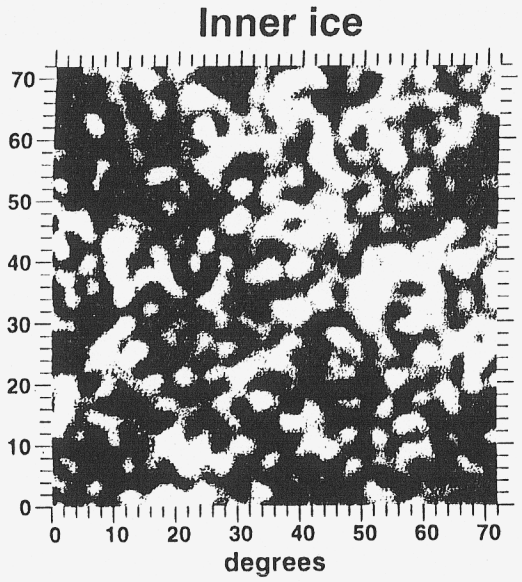
Inner ice
70
60
50
40
30
20
10
0
0 10 20 30 40 50 60 70
degrees

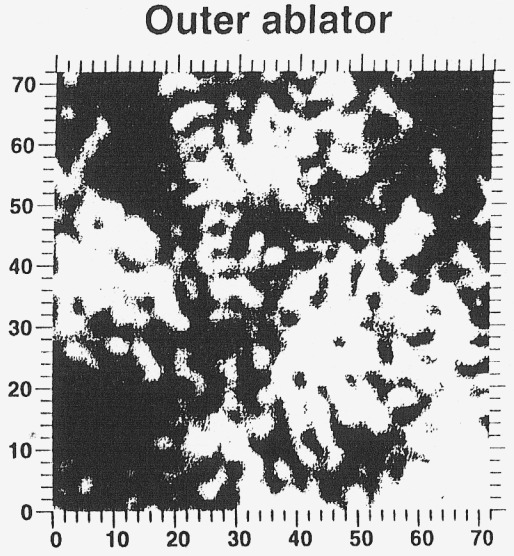
Outer ablator
70
60
50
40
30
20
10
0
0 10 20 30 40 50 60 70